

# Classical phase boundary location with information-theoretic entropy in tensor renormalization group flows

Adil A. Gangat<sup>1,2,3</sup> and Ying-Jer Kao<sup>1,4,5,\*</sup>

<sup>1</sup>*Department of Physics, National Taiwan University, Taipei 10607, Taiwan*

<sup>2</sup>*Dpartement de Physique, Universit de Sherbrooke, Sherbrooke, Qubec, Canada J1K 2R1*

<sup>3</sup>*School of Physics, Georgia Institute of Technology, Atlanta, GA 30332, USA*

<sup>4</sup>*National Center for Theoretical Sciences, National Tsing Hua University, Hsinchu 30013, Taiwan*

<sup>5</sup>*Department of Physics, Boston University, Boston, Massachusetts 02215, USA*

(Dated: December 15, 2024)

We present a simple and efficient tensor network method to accurately locate phase boundaries of two-dimensional classical lattice models. The method utilizes only the information-theoretic (von Neumann) entropy of quantities that automatically arise along tensor renormalization group [Phys. Rev. Lett. **12**, 120601 (2007)] flows of partition functions. We benchmark the method against theoretically known results for the square-lattice  $q$ -state Potts models and Monte Carlo results for the frustrated square lattice  $J_1 - J_2$  Ising model. We find good agreement in all cases, which includes first-order, weakly first-order, and continuous phase transitions, with much less computational cost than Monte Carlo methods.

## I. INTRODUCTION

Accurate numerical location of phase boundaries in two-dimensional classical lattice models is of wide interest. Monte Carlo methods can be used for this, but tensor network methods may be of utility as an independent check of Monte Carlo results or in cases where Monte Carlo methods become difficult. Tensor network methods for phase boundary location of classical lattice models entail analysis of either thermodynamic<sup>1</sup> or information-theoretic<sup>2-5</sup> quantities; here we are concerned with information-theoretic (von Neumann) entropy. A few recent works<sup>4-7</sup> have utilized von Neumann entropy to locate phase boundaries with the corner transfer matrix renormalization group (CTMRG) algorithm<sup>8,9</sup>. However, we are not aware of any works that have investigated this approach with the Tensor Renormalization Group (TRG)<sup>10</sup> algorithm. In this report we explain the straightforward use of von Neumann entropy for phase boundary location with the TRG algorithm, and we benchmark the method against theoretical results for the locations of first-order, weakly first-order, and continuous phase transitions. We also benchmark against Monte Carlo results for the phase boundary of a frustrated model.

The TRG algorithm is an algorithm for successive real space course graining of two-dimensional tensor networks. Partition functions of two-dimensional classical lattice models with local interactions can be represented as two-dimensional tensor networks<sup>10</sup>, and the TRG algorithm can therefore course grain such partition functions so that they become computationally feasible to evaluate in the thermodynamic limit. As part of the original TRG algorithm, a discrete, positive definite spectrum (“singular value spectrum”) is automatically generated at each course graining step. The method that we present below only requires computation of the von Neumann entropy of this singular value spectrum at each course graining step; it does not require computation of any thermodynamic quantities. Our method entails multiple TRG flows (which may occur in parallel), each at a different temperature. A simple analysis of the von Neumann entropy along

each TRG flow reveals which flow is occurring closest to the phase boundary. We show that this method works well for determining transition temperatures of first-order phase transitions, weakly first-order phase transitions, and continuous phase transitions. The method is accurate even in the case of large course graining errors along the TRG flows (as necessarily happens near criticality<sup>10</sup>). We note that this TRG-based method is in sharp contrast to the more costly approach of calculating thermodynamic quantities to high accuracy with TRG or higher-order TRG (HOTRG)<sup>11</sup>, as in Ref. 1. We also note that it is far cheaper than Monte Carlo methods.

## II. TRG FLOWS OF PARTITION FUNCTIONS NEAR PHASE BOUNDARIES

Partition functions of two-dimensional classical lattices can be represented as contractions of two-dimensional networks of tensors<sup>10</sup> where each tensor corresponds to a few lattice sites. An example given in Ref. 10 for the partition function ( $Z$ ) of a honeycomb lattice model is

$$Z = \sum_{ijk\dots} A_{ijk} A_{ilm} A_{jnp} A_{kqr} \dots, \quad (1)$$

where  $A_{ijk}$  is a three-leg tensor corresponding to three microscopic degrees of freedom. The TRG algorithm begins with a few (or even just one) tensors at the UV scale and applies a succession of steps, each of which simultaneously grows and coarse grains the lattice. The growth of the lattice is exponential in the number of TRG steps, which makes calculation of the thermodynamic partition function computationally feasible: after tens of TRG steps, a single tensor represents many degrees of freedom rather than just a few, and tracing over only a few (or sometimes even one) tensor becomes sufficient to approximate the partition function in the thermodynamic limit. For example, in the case of a monopartite square lattice the TRG algorithm may start with a single tensor corresponding to a system size of  $2 \times 2$ , and after  $N$  TRG steps end with a single tensor that corresponds to a system size of  $2^N \times 2^N$ .

TRG course graining entails an information compression scheme, based on the singular value decomposition, that in many cases allows the course grained tensors of a partition function to have low compression error (a.k.a. “truncation error”) while still keeping the dimension of their indices (a.k.a. “bond dimension”) within computationally feasible limits. More precisely, the minimum bond dimension required for maintaining low truncation error grows with each course graining step in the early part of the TRG flow of a partition function, but saturates to a finite value when the course graining approaches the correlation length of the system. Near criticality, however, the correlation length diverges, and TRG breaks down in the sense that the minimum bond dimension required for keeping low truncation error grows without saturating at a computationally feasible value. TRG course graining to the thermodynamic limit with low truncation error therefore becomes computationally prohibitive for partition functions near criticality (i.e. the tensors required become too large). Similarly, the finite but very large correlation lengths that are a hallmark of *weakly* first-order phase transitions can also make low-loss TRG flows to the thermodynamic limit computationally prohibitive. Crucially, *our method of using TRG flows to locate phase boundaries does not require the TRG flows to always maintain low truncation error*. Therefore, TRG flows with bond dimension ( $\chi$ ) fixed at computationally modest sizes are sufficient for our method.

### III. TRG VON NEUMANN ENTROPY AS GROUND STATE ENTANGLEMENT ENTROPY

The correspondence between 2d classical and (1+1)d quantum systems means that a theoretical understanding of our method can be gained by considering the entanglement properties of ground states of (1+1)d quantum spin chains and their finite- $\chi$  tensor network representations. We discuss here the specific case of matrix product states (MPSs)<sup>12–16</sup> due to the availability of relevant results. The wavefunction of an open boundary (1+1)d quantum spin chain with  $N$  sites may be represented as a MPS:  $|\Psi\rangle = \sum_{s_1, \dots, s_N=1}^d \text{Tr}(A_1^{s_1} \dots A_N^{s_N}) |s_1 \dots s_N\rangle$ , where the  $A_j$  are tensors of dimension  $d \times \chi \times \chi$ ,  $d$  is the dimension of spin  $s_j$  at site  $j$ , and  $\chi$  is again referred to as the “bond dimension”. The MPS representation of chains with periodic boundaries or infinite size is very similar.

For a bipartite quantum system  $AB$  in a pure state, the subsystems  $A$  and  $B$  may each still have a mixed (i.e. uncertain) state due to quantum correlations (i.e. entanglement) between  $A$  and  $B$ . The resulting “entanglement entropy” of subsystem  $A$  is defined as  $S = -\text{tr}(\rho_A \log_2 \rho_A)$ . It is useful to consider the entanglement entropy of a contiguous subblock in both infinite and finite (1+1)d quantum spin chains. In the ground state of the chain, the entanglement entropy of such a contiguous subblock, as well as its MPS representation, exhibits universal properties near and at criticality<sup>17–26</sup>.

In the ground state of an infinite chain, the entanglement entropy of the infinite half-chain diverges near criticality as  $S \propto \log(\xi)$ , where  $\xi$  is the correlation length of the system. In

an infinite MPS (iMPS)<sup>15,16</sup> representation, however, the finite bond dimension causes the entanglement entropy to saturate to a finite maximum near the critical point (the distance from the critical point goes to zero as  $\chi \rightarrow \infty$ )<sup>24,25</sup>. The finite  $\chi$  of iMPSs also leads to a  $\chi$ -dependent universal scaling behavior of local observables, which enables a “finite entanglement scaling” (FES)<sup>24,25</sup> analysis analogous to the well-known finite size scaling (FSS) analysis.

A finite-length ( $L$ ) contiguous subblock of an infinite chain has entanglement entropy constant in  $L$  off criticality and logarithmic in  $L$  at criticality (for sufficiently large  $L$ )<sup>20</sup>. This behavior also occurs for contiguous subblocks of sufficiently large *finite* chains in the ground state<sup>20</sup>, but with a modification: at criticality the entanglement entropy grows logarithmically over a finite range of  $L$  but then saturates and starts to decrease after reaching half the chain length due to the finiteness of the system. Thus, in either case (infinite chain or large, finite chain), there is a range of  $L$  for which the entanglement entropy is maximal at the critical point. For finite chains, MPS representations with sufficiently large  $\chi$  can reproduce this behavior. Further, it was shown for the case of periodic boundary conditions that such finite MPSs exhibit a crossover (as a function of  $\chi$  and system size) between regimes where either FSS or FES is valid<sup>26</sup>. For the entanglement entropy this means a crossover between  $S \propto \log(L)$  and  $S \propto \log(\chi)$ .

The upshot is that in all of the above cases of (1+1)d quantum systems and their finite-entanglement (i.e. finite- $\chi$ ) tensor network representations, the critical point can be approximately identified with the parameter value that maximizes the entanglement entropy. The same must also be true for first order transitions if the correlation length on both sides of the transition is maximal at the transition (this is intuitively expected to be the usual case). In the present work, we wish to investigate how well this information-theoretic way of locating phase boundaries of (1+1)d quantum systems translates to two-dimensional classical lattice models via the classical-quantum correspondence in TRG.

The classical-quantum correspondence in the case of TRG is such that the tensor at each step in a TRG flow of a classical 2d partition function corresponds to a representation of a (1+1)d quantum ground state imagined to live on the boundary of the classical system<sup>10</sup>. The gap of the corresponding classical and quantum systems is the same, and each tensor leg corresponds to a contiguous subblock of the periodic (1+1)d quantum system whose size grows exponentially in the number of TRG steps. For the example of a square lattice, this can be summarized as

$$|\Psi\rangle \approx \sum_{ijkl} A_{ijkl} |\psi_i\rangle |\psi_j\rangle |\psi_k\rangle |\psi_l\rangle, \quad (2)$$

where  $|\Psi\rangle$  is the boundary ground state wavefunction,  $A_{ijkl}$  is the TRG tensor, and  $|\psi_i\rangle$  is a pure state of the contiguous subblock corresponding to tensor leg  $i$ . Here it is manifest that the TRG tensor encodes the entanglement between the subblocks of the (1+1)d quantum chain. At each TRG step, a singular value spectrum results from a singular value decomposition of the reshaped tensor, e.g.  $A_{(ij)(kl)}$ . Therefore, the von Neumann entropy of the singular value spectrum at a par-

ticular TRG step corresponds to the entanglement entropy of a contiguous subblock of the boundary (1+1)d quantum system at that step. This is also the case for HOTRG<sup>27</sup>.

Near criticality the finite value of  $\chi$  results in a crossover in the behavior of the entanglement entropy growth from linear to constant in TRG step (see Fig. (1) for an example); this is qualitatively like the FSS to FES crossover known for periodic MPS<sup>26</sup> and also the scaling crossover near criticality in CTMRG<sup>28</sup>. Further, Ueda et al.<sup>27</sup> *quantitatively* confirmed the presence of FES in HOTRG flows of the critical partition function of the Ising model in the region after the crossover. We therefore make the following conjecture: FES is generically valid after the von Neumann entropy crossover in TRG flows of critical partition functions. Combining this conjecture with the behavior of entanglement in the FES regime of (1+1)d quantum systems, we arrive at the simple idea behind the method described in the next section: the maximum of the TRG von Neumann entropy after the crossover gives a good approximation for the location of the phase boundary. The benchmarks below validate this idea.

It seems surprising that (HO)TRG could retain any properties of criticality after the lattice is grown through the entropy scaling crossover because the crossover coincides with the onset of large truncation error; a partial explanation is that the saturation value of the entanglement entropy after the crossover necessarily depends on the slope of the entanglement entropy before the crossover (i.e. in the FSS regime), which in turn is determined by the central charge of the critical point. So, different  $\chi$  yield different saturation values of the entanglement entropy in (HO)TRG flows of critical partition functions, but the value of the difference is determined by the central charge. We also note here the result in Ref. 26 that ground states of critical MPS rings in the FES regime correctly capture local universal properties but have vanishing overlap with the true ground states.

#### IV. METHOD

In our simulations we always find that the von Neumann entropy of singular values in TRG flows of partition functions reaches a maximum along the flow just before plateauing in the FES regime (see Fig.(1) for an example). Though larger lattice sizes (i.e. more TRG steps) intuitively give better results in the absence of truncation error, it is of no benefit to grow the lattice further in a finite- $\chi$  simulation once the FES regime is reached since the correlation length has then reached the limit set by  $\chi$ . The number of TRG steps  $N$  after which the FES regime is entered is model- and  $\chi$ -dependent, but the generic existence of the entropy peak along TRG flows allows us to accommodate all scenarios in an algorithmically simple way. Therefore, for the sake of both accuracy and simplicity, our method is based around the peak value of the von Neumann entropy along individual TRG flows. Algorithmically, for the TRG flow at a given temperature and  $\chi$  we simply monitor the von Neumann entropy along the flow and find the step  $N_{\text{peak}}$  after which the von Neumann entropy decreases for five consecutive steps. We then record the von Neumann

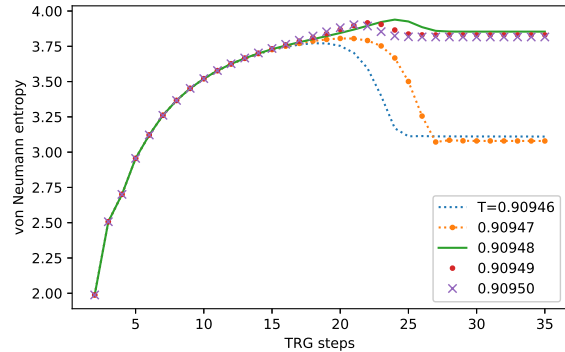


FIG. 1. von Neumann entropy of the singular value spectrum along TRG flows of the partition function at different temperatures near criticality for the  $q = 4$  Potts model on the square lattice. The bond dimension chosen here is  $\chi = 20$ . For a given  $\chi$ , the temperature that maximizes the entropy peak (in this case  $T = 0.90948$ , solid line) is designated as the transition temperature.

entropy at step  $N_{\text{peak}}$  as the peak entropy value for that temperature and  $\chi$ . For a given  $\chi$ , the temperature that maximizes this peak entropy is designated as the transition temperature. For first order transitions there is no emergent criticality or FES regime, but with the assumption that the physical correlation length is still maximal at the phase boundary we prescribe the same method. We show with benchmarks below that this method works very well with only modest  $\chi$  for continuous, weakly first order, and regular first order phase transitions, and that it works for both unfrustrated and frustrated systems.

#### V. BENCHMARK: POTTS MODELS

Here we benchmark our method with theoretical results for the  $q$ -state Potts models on the square lattice<sup>32</sup>; the Hamiltonian is

$$\mathcal{H} = -J \sum_{\langle i,j \rangle} \delta_{\sigma_i, \sigma_j}, \quad (3)$$

where  $J > 0$ ,  $\delta$  is the Kronecker delta function,  $\langle \rangle$  denotes nearest neighbors, and  $\sigma = 1, 2, \dots, q$ . For  $q \leq 4$  the phase transition is theoretically known as continuous, and for  $q > 4$  it is first-order. For  $q = 5$  the phase transition is very weakly first order (i.e. has a finite but very large correlation length); the strength of the first order nature increases with  $q$  (i.e. the correlation length becomes smaller).

In Table I we compare the transition temperatures found with our method (to precision  $10^{-5}$ ) with the theoretically known values  $T^* = (J/k_B)/\ln(1 + \sqrt{q})$ . Our method performs very well with only moderate values of  $\chi$ , and the numerical results get closer to the theoretical results as  $\chi$  increases.

TABLE I. Numerical and theoretical phase transition temperatures for the  $q$ -state Potts models on the square lattice.  $\xi$  is the theoretically known correlation length<sup>29,30</sup> at the transition (when approached from the higher temperature phase). The numerical values are obtained with our TRG von Neumann entropy method to five decimal places with different values of the bond dimension  $\chi$ . There is good agreement with the theoretically known values.

q-state Potts sq. lattice	$q = 3$ ( $\xi = \infty$ )	$q = 4$ ( $\xi = \infty$ )	$q = 5$ ( $\xi = 2512.2$ )	$q = 6$ ( $\xi = 158.9$ )	$q = 10$ ( $\xi = 10.6$ )
TRG, $\chi=20$	0.99795	0.90948	0.85035	0.80908	0.70553
TRG, $\chi=30$	0.99453	0.91144	0.85099	0.80647	0.70255
TRG, $\chi=40$	0.99486	0.91082	0.85193	0.80713	0.70252
theory	0.99497	0.91024	0.85153	0.80761	0.70123

TABLE II. Numerical phase transition temperatures for the  $J_1 - J_2$  Ising model on the square lattice as determined with our TRG von Neumann entropy method to two decimal places and with Monte Carlo in Ref. 31. The quoted Monte Carlo values are approximated from the plot in Fig. (3) in Ref. 31. Our method is computationally much cheaper, but gives results in agreement with Monte Carlo.

$J_1$ - $J_2$ sq. lattice	$\frac{J_2}{ J_1 } = 0.1$	$\frac{J_2}{ J_1 } = 0.3$	$\frac{J_2}{ J_1 } = 0.4$	$\frac{J_2}{ J_1 } = 0.6$	$\frac{J_2}{ J_1 } = 0.8$
TRG, $\chi=20$	1.94	1.25	0.95	0.97	1.57
TRG, $\chi=30$	1.94	1.25	0.95	0.97	1.57
Monte Carlo	$\sim 1.9$	$\sim 1.25$	$\sim 0.9$	$\sim 0.95$	$\sim 1.55$

## VI. BENCHMARK: J1-J2 ISING MODEL

Here we benchmark our method with previous Monte Carlo results for the (frustrated)  $J_1 - J_2$  Ising model on the square lattice. The Hamiltonian is

$$\mathcal{H} = J_1 \sum_{\langle i,j \rangle} \sigma_i \sigma_j + J_2 \sum_{\langle\langle i,j \rangle\rangle} \sigma_i \sigma_j, \quad (4)$$

where  $\sigma = \uparrow, \downarrow$ ,  $\langle \rangle$  denotes nearest neighbors, and  $\langle\langle \rangle\rangle$  denotes next nearest (i.e. diagonal) neighbors. The corresponding partition function can be expressed as a contraction of a tensor network on the dual lattice such that the tensor bonds correspond to link variables instead of spin variables; for details we refer the reader to Ref. 33.

In Table II we compare the transition temperatures found with our method (to precision  $10^{-2}$ ) with the values obtained in the Monte Carlo study in Ref. 31. With only moderate values of  $\chi$ , the results from our method match closely with the Monte Carlo results. We note that Monte Carlo becomes more difficult for this model near the point  $J_2/|J_1| = 0.5$  due to the presence of many coexisting phases there<sup>31</sup> while our TRG method remains unaffected.

## VII. DISCUSSION

By leveraging the 2d classical to (1+1)d quantum correspondence known for TRG and what is already known about the behavior of the entanglement entropy in MPSs near criticality, we have shown that the von Neumann entropy in com-

putationally efficient TRG flows of partition functions near first-order, weakly first-order, and continuous phase transitions can provide an accurate determination of phase transition temperatures inspite of the presence of large truncation errors.

An alternative information-theoretic method of phase boundary location with (HO)TRG was introduced in Ref. 2, where the degeneracy of the phase is extracted from the fixed point tensor and the phase boundary is identified with an abrupt change in the degeneracy. In some cases that method may suffer from issues of instability that obscure the location of the phase boundary, as seen in Ref. 3, which the method presented here does not suffer from. Further, the degeneracy signal used in the other method usually remains constant within a phase, while the von Neumann entropy used in the present method usually increases (roughly) monotonically as the phase boundary is approached and therefore makes it easier to locate the phase boundary.

Due to its combination of simplicity, efficiency, and accuracy, the method reported here has the potential to become a standard tool for locating phase boundaries of 2d classical lattice models. An open question is whether or not any benefit can be gained by substituting TRG with HOTRG in this method.

## VIII. ACKNOWLEDGEMENTS

AAG acknowledges discussions with Kai-Hsin Wu and Glen Evenbly. This work is supported by the MOST in Taiwan through Grants No. 107-2112-M-002 -016 -MY3, and 105-2112-M-002 -023 -MY3.

\* yjkao@phys.ntu.edu.tw

<sup>1</sup> S. Morita and N. Kawashima, arXiv preprint arXiv:1806.10275 (2018).



- <sup>2</sup> Z.-C. Gu and X.-G. Wen, *Phys. Rev. B* **80**, 155131 (2009).
- <sup>3</sup> L.-P. Yang and Z.-Y. Xie, *J. Phys. Soc. Jpn.* **85**, 104602 (2016).
- <sup>4</sup> R. Krčmár and L. Šamaj, *Phys. Rev. E* **92**, 052103 (2015).
- <sup>5</sup> C.-Y. Huang, T.-C. Wei, and R. Orús, *Phys. Rev. B* **95**, 195170 (2017).
- <sup>6</sup> R. Krčmar, A. Gendiar, and T. Nishino, *Phys. Rev. E* **94**, 022134 (2016).
- <sup>7</sup> R. Krčmár, A. Gendiar, and T. Nishino, arXiv preprint arXiv:1612.07611 (2016).
- <sup>8</sup> T. Nishino and K. Okunishi, *J. Phys. Soc. Jpn.* **65**, 891 (1996).
- <sup>9</sup> T. Nishino and K. Okunishi, *J. Phys. Soc. Jpn.* **66**, 3040 (1997).
- <sup>10</sup> M. Levin and C. P. Nave, *Phys. Rev. Lett.* **99**, 120601 (2007).
- <sup>11</sup> Z.-Y. Xie, J. Chen, M.-P. Qin, J. W. Zhu, L.-P. Yang, and T. Xiang, *Phys. Rev. B* **86**, 045139 (2012).
- <sup>12</sup> M. Fannes, B. Nachtergaele, and R. F. Werner, *Comm. Math. Phys.* **144**, 443 (1992).
- <sup>13</sup> S. Östlund and S. Rommer, *Phys. Rev. Lett.* **75**, 3537 (1995).
- <sup>14</sup> D. Perez-Garcia, F. Verstraete, M. Wolf, and J. Cirac, *Quantum Inf. Comput.* **7** (2007).
- <sup>15</sup> G. Vidal, *Phys. Rev. Lett.* **98**, 070201 (2007).
- <sup>16</sup> R. Orus and G. Vidal, *Phys. Rev. B* **78**, 155117 (2008).
- <sup>17</sup> L. Amico, R. Fazio, A. Osterloh, and V. Vedral, *Rev. Mod. Phys.* **80**, 517 (2008).
- <sup>18</sup> C. Holzhey, F. Larsen, and F. Wilczek, *Nucl. Phys. B* **424**, 443 (1994).
- <sup>19</sup> A. Osterloh, L. Amico, G. Falci, and R. Fazio, *Nature* **416**, 608 (2002).
- <sup>20</sup> G. Vidal, J. I. Latorre, E. Rico, and A. Kitaev, *Phys. Rev. Lett.* **90**, 227902 (2003).
- <sup>21</sup> J. I. Latorre, E. Rico, and G. Vidal, arXiv preprint quant-ph/0304098 (2003).
- <sup>22</sup> P. Calabrese and J. Cardy, *J. Stat. Mech. Theory Exp.* **2004**, P06002 (2004).
- <sup>23</sup> G. Refael and J. E. Moore, *Phys. Rev. Lett.* **93**, 260602 (2004).
- <sup>24</sup> L. Tagliacozzo, T. R. de Oliveira, S. Iblisdir, and J. Latorre, *Phys. Rev. B* **78**, 024410 (2008).
- <sup>25</sup> F. Pollmann, S. Mukerjee, A. M. Turner, and J. E. Moore, *Phys. Rev. Lett.* **102**, 255701 (2009).
- <sup>26</sup> B. Pirvu, G. Vidal, F. Verstraete, and L. Tagliacozzo, *Phys. Rev. B* **86**, 075117 (2012).
- <sup>27</sup> H. Ueda, K. Okunishi, and T. Nishino, *Phys. Rev. B* **89**, 075116 (2014).
- <sup>28</sup> T. Nishino, K. Okunishi, and M. Kikuchi, *Phys. Lett. A* **213**, 69 (1996).
- <sup>29</sup> E. Buddenoiir and S. Wallon, *J. Phys. A Math. Gen.* **26**, 3045 (1993).
- <sup>30</sup> S. Iino, S. Morita, A. W. Sandvik, and N. Kawashima, arXiv preprint arXiv:1801.02786 (2018).
- <sup>31</sup> A. Kalz, A. Honecker, S. Fuchs, and T. Pruschke, *Eur. Phys. J.* **65**, 533 (2008).
- <sup>32</sup> F.-Y. Wu, *Rev. Mod. Phys.* **54**, 235 (1982).
- <sup>33</sup> H.-H. Zhao, Z.-Y. Xie, Q. N. Chen, Z.-C. Wei, J. W. Cai, and T. Xiang, *Phys. Rev. B* **81**, 174411 (2010).